



ELSEVIER

Available online at www.sciencedirect.com

SCIENCE @ DIRECT®

Journal of Nuclear Materials 321 (2003) 184–191

Journal of
nuclear
materials

www.elsevier.com/locate/jnucmat

Parametric study of a corrosion model applied to lead–bismuth flow systems [☆]

Jinsuo Zhang ^{*}, Ning Li

Los Alamos National Laboratory, Los Alamos, NM 87545, USA

Received 9 September 2002; accepted 21 April 2003

Abstract

The corrosion of steels exposed to flowing liquid metals is influenced by local and axial conditions of the flow systems. Despite of this, most existing corrosion models only consider the mean values based on local conditions. The present study refines a model for flowing liquid metal under non-isothermal conditions. The model is based on solving the mass transport equation in the boundary layer. Two kinds of flows are investigated: through an open pipe system and through a closed loop system. The model is applied to a lead–bismuth eutectic (LBE) test loop. A parametric study illustrates the effects of the axial temperature profile on corrosion. The study provides important insight to the design, operation and testing of such loop systems.

© 2003 Elsevier B.V. All rights reserved.

1. Introduction

Corrosion of containment and structural materials presents a critical challenge in the use of liquid lead–bismuth eutectic (LBE) or lead as a nuclear coolant in accelerator-driven systems and advanced reactors. Properly controlling the oxygen activity in LBE to mitigate corrosion proves effective under certain conditions. Liquid metal corrosion can proceed via dissolution at very low oxygen concentration, and through surface oxidation and reduction of surface oxides at higher oxygen concentrations. Corrosion rate is typically a function of local temperature and flow velocity. However, corrosion and precipitation rates and profiles can depend strongly on the axial temperature profile, limiting the applicability of many corrosion models.

The majority of corrosion research focuses on the influence of the local conditions, in particular the ve-

locity of the liquid and the local temperature. The axial temperature profile, or the axial profile of the boundary concentration of the corrosion product, is usually neglected in the analysis of corrosion kinetics. The corrosion rate q is calculated using the following equation [1]:

$$q = K(c_s - c_b), \quad (1)$$

where K is the mass transfer coefficient dependent on the flow velocity, c_s is the corrosion product concentration at the liquid–solid interface dependent on the local temperature, and c_b is the concentration in the bulk flow and is often set to $c_b \approx 0$ [1]. Based on the above equation, the corrosion rate is determined by the hydrodynamic parameters and the local temperature. However, many industrial flow systems subject to corrosion are under non-isothermal conditions, and the axial temperature profile may have a profound effect on the rate of material corrosion. As a result, an accurate description of the corrosion phenomena that take place in a non-isothermal system can be accomplished only if the axial conditions are taken into consideration.

Regarding the axial temperature profile effects, Epstein [2] developed a model that could be used to calculate the mean corrosion rate at the hot zone in heat

[☆] This research is supported by Department of Energy under contact number W-7405-ENG-36.

^{*} Corresponding author. Tel.: +1-505 667 7444; fax: +1-505 665 2659.

E-mail address: jzhang@cnls.lanl.gov (J. Zhang).

transfer loops. A kinetic model, only taking into account the phenomena of dissolution–deposition, liquid state diffusion and transport of the dissolved metal in liquid metal, was developed by Sannier and Santarini [3] to study corrosions in a natural convection lead loop. Employing the model, the authors obtained good results consistent with their experimental results, indicating that the model has high performance and can be used to predict corrosion rate in some loop systems. However, the author assumed that the mass transfer boundary layer is only a function of the liquid metal velocity and remains the same thickness along the loop. This assumption is reasonable when the surface concentration or temperature gradient is small (in their loop, the temperature difference is 80 K), but for a loop system with large surface concentration or temperature gradient that is often encountered in engineering applications, more sophisticated model needs to be developed.

Another kinetic model incorporating the effects of the axial temperature profile has been developed by He et al. [4]. The model demonstrates that the axial temperature profiles have significant effects on corrosion and precipitation phenomena. However, this model is limited for simple loop flows, and there is a missing term in the solution of the boundary layer concentration.

Following the approach presented in Ref. [4], the present study extends the kinetic model for loop flows to more general cases. We first derive a kinetic solution by solving the governing concentration equation in the boundary layer. Two types of flows are examined: a closed loop flow and an open pipe flow. From the non-local analysis, we elucidate the difference of the corrosion phenomena between the closed loop flow and the open pipe flow. We also investigate the effects of axial temperature profiles on the profile of the corrosion and precipitation. This information will be very useful for the design and operation of liquid metal flow systems.

2. Theory

2.1. Analytical solution

In general, the following convection–diffusion equation is used to calculate the mass transport in flowing liquid system:

$$\frac{\partial c}{\partial t} + (\vec{u} \cdot \nabla)c = D\nabla^2 c + q, \quad (2)$$

where c is the concentration of the corrosion product under study, \vec{u} is the velocity vector field of the liquid, D is the mass diffusion coefficient, and q is the net production (consumption) rate due to chemical reactions in the liquid. In the present study, we adopt the following assumptions:

- (1) The reaction term contributes little to the mass transfer in bulk fluids, or $q = 0$;
- (2) The flow is fully turbulent. Therefore, it is reasonable to assume that the mixing flow homogenizes the bulk concentration.
- (3) The fluid media is liquid metal, so the diffusion coefficient is much smaller than the kinematic viscosity. The Schmidt number ($Sc = \nu/D$, where ν is the kinematic viscosity) is very large.
- (4) The physical properties of the flowing liquid and the bulk flow velocity stay constant along the axis of the loop.
- (5) The wall surface is smooth and the corrosion and precipitation do not change the wall surface enough to affect the fluid flow.

Based on the assumptions, the variation of the corrosion product concentration is confined in a thin incompressible boundary layer, where convection is dominant in the longitudinal direction (flow direction) and diffusion is dominant in the transverse direction. For the steady state case, the governing equation in the boundary layer can be written as

$$u \frac{\partial c}{\partial x} = D \frac{\partial^2 c}{\partial y^2}, \quad (3)$$

where x and y are coordinates in the axial and transverse directions, respectively.

The higher the value of Sc , the thinner the diffusion layer will be. For this case, the velocity boundary layer thickness is large compared to the species mass transfer boundary layer. It is conventional to approximate that the velocity is linear in the transverse coordinate y in the diffusion layer, that is

$$u = \gamma y, \quad (4)$$

where $\gamma = \lambda V^2/2\nu$, λ is the Fanning friction factor and V is the bulk flow velocity outside the boundary layer. Introducing

$$\xi = \frac{x}{L}, \quad \eta = \left(\frac{\gamma}{DL}\right)^{1/3} y,$$

where L is the reference length (loop/pipe length) in the main flow direction, the following dimensionless equation is obtained:

$$\eta \frac{\partial c}{\partial \xi} = \frac{\partial^2 c}{\partial \eta^2}. \quad (5)$$

The boundary condition is:

$$\text{At } \eta = 0, \quad c_w = c_w(\xi) \quad (6)$$

and the concentration in the bulk flow is finite with a mean value c_0^b . Now we expand the concentration in a Fourier series

$$c = \sum_k Y_k(\eta) \exp(2\pi k i \xi). \quad (7)$$

We also expand the concentration at the wall into a Fourier series

$$c_w = \sum_k c_k \exp(2\pi k i \xi). \quad (8)$$

Each Fourier harmonics, $Y_k(\eta)$, satisfies the following ODE:

$$2k\pi i \eta Y_k(\eta) = \frac{d^2 Y_k(\eta)}{d\eta^2}. \quad (9)$$

For $k = 0$, the solution of Eq. (9) is

$$Y_0(\eta) = \frac{(c_0^b - c_0)}{\delta_D} \left(\frac{DL}{\gamma} \right)^{1/3} \eta + c_0, \quad (10)$$

where δ_D is the thickness of concentration boundary layer for the constant surface concentration and c_0 is the mean wall concentration.

For $k > 0$, the solution of Eq. (9) is

$$Y_{k>0}(\eta) = a_k Ai((2\pi k i)^{1/3} \eta) + b_k Bi((2\pi k i)^{1/3} \eta), \quad (11)$$

where Ai and Bi are Airy functions. Considering the boundary condition, we obtain

$$b_k = 0, \quad a_k = \frac{c_k}{Ai(0)}, \quad (k \neq 0).$$

For $k < 0$, since the concentration is real, $Y_{k<0}(\eta) = \bar{Y}_{|k|}(\eta)$, where the bar represents the conjugate term. Then the solution of Eq. (3) is

$$c = \frac{(c_0^b - c_0)}{\delta_D} \left(\frac{DL}{\gamma} \right)^{1/3} \eta + c_0 + \sum_{k>0} Y_k(\eta) \exp(2\pi k i \xi) + \sum_{k<0} \bar{Y}_{|k|}(\eta) \exp(2\pi k i \xi), \quad (12)$$

where $Y_{k>0}(\eta) = a_k Ai((2\pi k i)^{1/3} \eta)$. The species flux $q(\xi)$ at the wall into the fluid can be calculated through the Fick's first law as:

$$q(\xi) = -D \frac{\partial c}{\partial y} \Big|_{y=0} = \frac{D}{\delta_D} (c_0 - c_0^b) + \left(\frac{2\pi D^2 \gamma}{3L} \right)^{1/3} \frac{1}{\Gamma(1/3)} \sum_{k \neq 0} Q_k \times \exp(2\pi k i \xi), \quad (13)$$

where Γ is the Gamma function, and $Q_k = a_k k^{1/3} i^{1/3}$ for $k > 0$ and $Q_k = a_k |k|^{1/3} (-i)^{1/3}$ for $k < 0$. When $q > 0$, the corrosion product flux is from the surface to the bulk liquid, corresponding to corrosion, while for $q < 0$, the flux is from bulk fluid to the surface, corresponding to deposition.

In Eqs. (12) and (13), the indices should be set more carefully. The imaginary unit i has three cube roots, that

is $i^{1/3} = (\sqrt{3}/2 + i/2, -\sqrt{3}/2 + i/2, -i)$. Regarding the boundary condition that the concentration c is finite when $\eta \rightarrow +\infty$ and the properties of the Airy function that $Ai(x)$ oscillates with x when $\text{Real}(x) < 0$ and approaches to zero when $\text{Real}(x) > 0$, it requires $\text{Real}((2\pi k i)^{1/3}) > 0$ for $k > 0$. So in the present solution $i^{1/3} = \sqrt{3}/2 + i/2$ and $(-i)^{1/3} = \sqrt{3}/2 + i/2$.

The $k = 0$ case is treated incorrectly in Ref. [4], leading to solutions without the typical mass transfer term that is only dependent on the mean quantities, while the profile dependent on axial conditions remains the same.

2.2. Solution for open pipe flow

Let us first consider a fully developed turbulent flow in an open isothermal pipe with a constant species concentration at the wall, that is $c_w = c_0$ and accordingly $a_k = 0$.

Based on Eq. (12), the solution of the concentration in the boundary layer is

$$c = \frac{(c_0^b - c_0)}{\delta_D} \left(\frac{DL}{\gamma} \right)^{1/3} \eta + c_0. \quad (14)$$

The above equation indicates that for an open isothermal pipe flow, the concentration in the mass transfer boundary layer is linear in the transverse coordinate y . From this equation,

$$q = \frac{D}{\delta_D} (c_0 - c_0^b) = K(c_0 - c_b), \quad (15)$$

where $K = D/\delta_D$ is the mass transfer coefficient, c_b is the bulk concentration and $c_b \approx 0$ [1].

Eq. (15) has been used by many authors to estimate the corrosion rate in flowing liquid systems. According to the above analysis, this equation can only be used for the isothermal condition, or equivalently a constant concentration at the boundary. The boundary layer has to be fully developed. Thus the application of Eq. (15) to isothermal sections in non-isothermal loops is limited.

For the non-isothermal cases, the corrosion rate should be calculated as

$$q = K(c_0 - c_0^b) + \left(\frac{2\pi D^2 \gamma}{3L} \right)^{1/3} \frac{1}{\Gamma(1/3)} \sum_{k \neq 0} Q_k \exp(2\pi k i \xi). \quad (16)$$

For these cases, the local corrosion rate is composed of two parts: the mean part and the part due to the axial concentration gradient along the wall.

2.3. Solution for closed loop flow

Because the liquid in a closed loop is not renewed, the total amount of corrosion should equal to the total

amount of precipitation in the entire loop at the steady state

$$\int_0^L q dx = 0, \tag{17}$$

where L is the loop length. Substituting Eq. (13) into Eq. (17), we find $c_0^b = c_0$. So the concentration in the boundary layer and the corrosion rate are:

$$c = c_0 + \sum_{k>0} Y_k(\eta) \exp(2\pi k i \xi) + \sum_{k<0} \bar{Y}_{|k|}(\eta) \exp(2\pi k i \xi), \tag{18}$$

$$q = \left(\frac{2\pi D^2 \gamma}{3L} \right)^{1/3} \frac{1}{\Gamma(1/3)} \sum_{k \neq 0} Q_k \exp(2\pi k i \xi). \tag{19}$$

For an isothermal closed loop, from Eq. (18), we find $c = c_0$, this means that there is no concentration gradient between the bulk flow and wall surface. So there is no corrosion in a closed isothermal loop at the steady state. For the non-isothermal closed loop case, the mean corrosion rate is zero, while local corrosion rate depends on the axial boundary concentration profile.

3. Analysis results

The above model is applied to a material test loop (MTL) in our Laboratory. The MTL is a non-isothermal closed loop and is used to study the corrosion of various materials in flowing LBE. It uses a recuperator, a heater and a heat exchanger to set and control the temperature profile. LBE comes out of the pump at a low temperature, passes through the recuperator shell side and the heater, and reaches the highest temperature at the test section. On the return path, the temperature decreases through the recuperator tube side and the heat exchanger, and reaches the lowest temperature. The temperature profile is shown in Fig. 1 [5].

In oxygen control LBE systems [6], we calculate the iron (the main corrosion product) concentration at the interface of LBE and the wall through the following equation [4]

$$c_w = \text{Min}(10^{6.01 - 4380/T}, c_0^{-4/3} 10^{11.35 - (12844/T)}), \tag{20}$$

where c_w is the surface concentration in ppm, c_0 is the oxygen concentration in LBE and T is the absolute temperature in Kelvin.

The following parameters are used in the analysis: loop/pipe length $L = 29.92$ m, hydraulic diameter $d = 0.0525$ m, kinematic viscosity of LBE $\nu = 1.5 \times 10^{-7}$ m² s⁻¹ [4], liquid LBE velocity $V = 0.5$ m s⁻¹, oxygen concentration in LBE $c_0 = 0.01$ ppm.

The diffusion coefficient of iron in LBE: $D_{\text{Fe} \rightarrow \text{Pb-Bi}} = 10^{-9}$ m² s⁻¹ (estimated based on data from Ref. [4]).

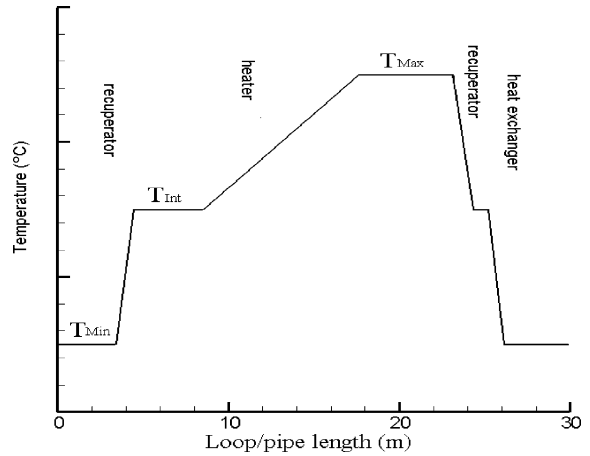


Fig. 1. Temperature profile of the LBE test loop (MTL).

The Blasius equation [1] is used to calculate the friction factor λ , that is

$$\lambda = 0.046 Re^{-0.20} \quad (Re = Vd/\nu).$$

There are several expressions [1] for the mass transfer coefficient K developed in aqueous media based on the experimental data. Balbaud-Celerier and Barbier [1] found that the expression developed by Berger and Hau [7] is the best one to estimate the corrosion rate in liquid metal systems. Therefore we use the Berger and Hau's expression which is

$$K_{B-H} = 0.0165 \nu^{-0.530} D^{0.670} V^{0.860} d^{-0.140}.$$

Three sets of the corrosion rates for pipe (hypothetically open) and closed loop flows based on the temperature profile are shown in Fig. 2 for $T_{\text{max}} = 550$ °C.

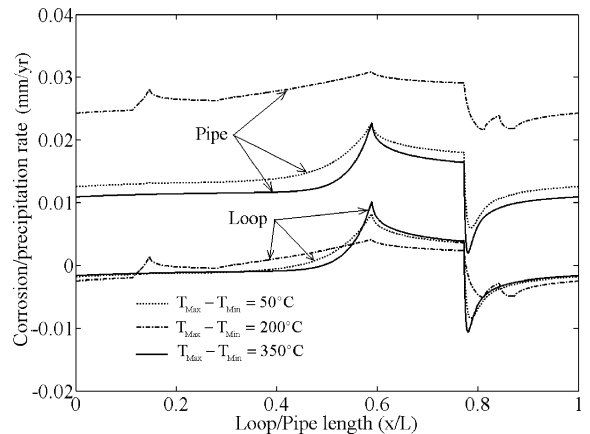


Fig. 2. Corrosion rate under three conditions ($T_{\text{max}} = 550$ °C, $T_{\text{int}} = (T_{\text{min}} + T_{\text{max}})/2$).

The figure illustrates the difference between the pipe and loop flow, and the effects of axial temperature profile on the profiles of the corrosion.

For this pipe flow, there is no precipitation (this is not a general conclusion for all cases, see Section 4), the maximal corrosion occurs at the beginning of maximal temperature, while the minimal corrosion is at the intermediate temperature and its position moves downstream as the temperature variation decreases. A smaller temperature gradient leads to higher corrosion rates and smaller variations.

For the closed test loop flow, the mean corrosion rate is zero. The integrated corrosion must equal to the integrated precipitation over the entire loop. The highest corrosion occurs at the beginning of loop section with the highest temperature, while the maximal precipitation takes place shortly after the temperature in the flow direction begins to decrease, and the location moves downstream as the temperature gradient decreases. Another difference between the pipe flow and loop flow is that a smaller temperature gradient leads to a smaller corrosion at the highest temperature section for the loop flow. The variation in the corrosion/precipitation rate becomes more significant as the temperature gradient increases. However, after the gradient exceeds a certain level, the corrosion/precipitation rate changes very little with any further increase of temperature gradient.

To illustrate the effects of the maximal temperature, as well as the temperature difference between the maximal temperature and the minimal temperature ($T_{\max} - T_{\min}$), on the corrosion rate at the test section, the surface plot of the mean corrosion rate in the hot test section as functions of the temperature difference and the maximal temperature is shown in Fig. 3. The corrosion rate increases with the temperature difference and the change slows after the difference exceeds 100 °C, and nearly saturates after reaching 200 °C. For the same

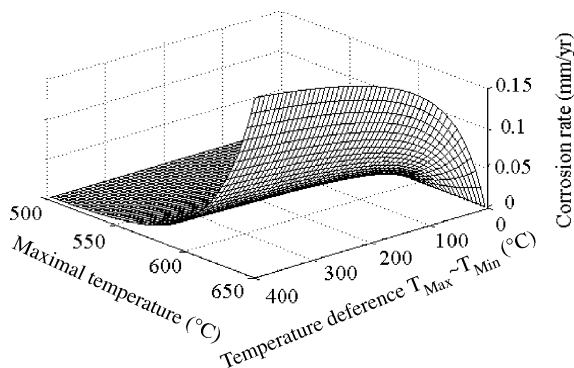


Fig. 3. The mean corrosion rate at the test section of the LBE loop as a function of the temperature gradient and the maximal temperature ($T_{\text{int}} = (T_{\text{min}} + T_{\text{max}})/2$).

gradient, the corrosion increases drastically with the maximal temperature. For accelerated corrosion testing, it is desirable to increase the testing temperature and set the temperature difference closer to 200 °C.

It is demonstrated that the corrosion/precipitation profile in a closed loop depends both on the axial boundary concentration gradient and the local boundary concentration. To illustrate the intermediate temperature effects, four corrosion/precipitation rates under different intermediate temperature for $T_{\max} = 550$ °C and $T_{\max} - T_{\min} = 200$ °C are shown in Fig. 4. The intermediate temperature has strong influence on corrosion/precipitation rates and profiles through changing the temperature and surface concentration gradients. With the increasing intermediate temperature, the corrosion rate in the maximal temperature section is reduced, while in the first intermediate temperature section (in the forward flow direction), the corrosion rate is increased, and in the second intermediate temperature section, the location for the highest precipitation moves downstream. For the test samples located in the maximal temperature section in the test loop, it is desirable to reduce the intermediate temperature to reduce the test time.

This new understanding of the dependence of corrosion/precipitation rates on the axial temperature profile is very useful for helping to design and operate non-isothermal closed loop systems. We plan to verify the key aspects in future experiments. This dependence implies that the corrosion test results obtained from one flow loop cannot be directly applied to another loop with a different temperature profile. It also suggests that it is possible to design flow systems to minimize corrosion and precipitation, or change the locations of maximal precipitation for enhanced system lifetime performance.

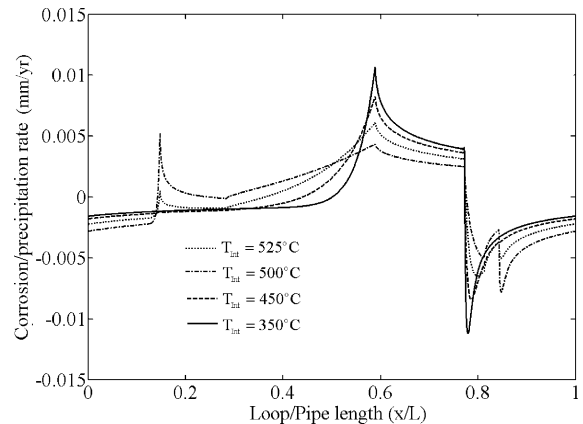


Fig. 4. Corrosion rate of the LBE loop for different intermediate temperatures ($T_{\max} = 550$ °C, $T_{\min} = 350$ °C).

4. Discussion

By solving the governing mass transport equation in the boundary layer with the assumptions that the convective transport dominates in the longitudinal flow direction and the mass diffusion dominates in the transverse direction, we develop a corrosion model for isothermal and non-isothermal flow system. The present study corrects a minor error and extends the previous work [4] to more general cases. It also explains why using the mean corrosion model would consistently lead to predicting larger corrosion rates in closed loops [1].

To elucidate the performance of the present model, the corrosion/precipitation profile for the pure lead natural convection loop set up by Sannier and Santarini [3] was calculated using the present model. All the parameters employed are the same to those in Ref. [3]. The corrosion/precipitation rate and temperature profile are shown in Fig. 5. In the experiment, the samples are installed in the highest temperature leg. The authors found the corrosion depth for steel 10 CD 9–10 is between 75 and 110 μm after 3000 h and for Z 10 CD Nb V 92 steel is between 25 and 40 μm after 2800 h. The present model predicts an iron corrosion depth between 40 and 70 μm after 3000 h. The deviations are probably expected due to experimental uncertainties and alloy composition effects.

Balbaud-Celerier and Barbier [1], using the local corrosion model and assuming the bulk iron concentration to be zero, examined the same pure lead loop and the predicted corrosion rate is about 239 μm after 3000 h, 2.1 times higher than the maximal experimental results. Through modeling the bulk corrosion product concentration, our previous study [8] incorporating the effects of the axial temperature profile, improves the

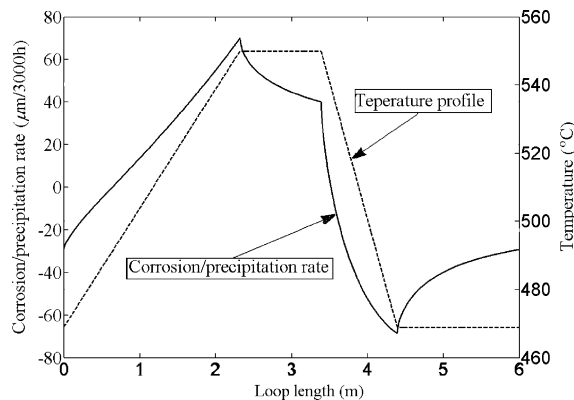


Fig. 5. Calculated corrosion/precipitation rate for the pure lead loop [3] and its temperature profile.

local model to be used in closed loop systems. The calculated corrosion rate for the pure lead loop is around 89 μm after 3000 which is close to the mean experimental rate for steel 10 CD 9–10. However, the improved local model can only give the mean corrosion rate at the hot zone, the present model provides the corrosion/precipitation profile and elucidates the ‘upstream’ and ‘downstream’ effect.

In Ref. [8], the mean corrosion rate at the highest temperature leg of MTL loop was calculated. The study provides the same dependence of the corrosion rate on the maximal temperature and the temperature difference between the maximal and minimal temperature, while the value is a little higher than the present result. Ref. [8] accounted for the axial temperature effects partly through modeling the bulk concentration. The ‘developing’ effects of the mass transfer boundary layer are neglected and therefore the model could only provide the mean corrosion/precipitation rate. In the present model, the convection–diffusion equation is solved in the mass transfer boundary. The non-local analyses show the corrosion/precipitation profile and what the maximal corrosion and precipitation rates are and where they are located.

To quantify the scaling dependence of the corrosion rate on hydrodynamic and transport parameters, the corrosion rate is rewritten in the following form:

$$q = \beta f(\xi) + K(c_0 - c_0^b). \quad (21)$$

The function $f(\xi)$ depends only on the boundary condition. The parameter β , which may be called the mass transfer coefficient for the loop corrosion rate, is defined by

$$\begin{aligned} \beta &= \frac{1}{\Gamma(1/3)Ai(0)} \left(\frac{2\pi D^2 \gamma}{3L} \right)^{1/3} \\ &= 0.3825 v^{-0.27} D^{0.667} \nu^{0.60} d^{-0.067} L^{-0.333}. \end{aligned} \quad (22)$$

The equation above indicates that the kinetic corrosion/precipitation rate is proportional to $V^{0.60}$, $d^{-0.067}$ and $L^{-0.333}$. Accordingly the local corrosion rate increases with the flow velocity, and decreases with the loop/pipe length for the same temperature difference, but depends little on the pipe diameter.

The mass transfer coefficient is usually expressed in a dimensionless form by the Sherwood number:

$$Sh = \frac{Kd}{D}.$$

We use the expression of the mass transfer coefficient developed by Berger and Hau [7], and obtain

$$Sh = 0.0165 Re^{0.860} Sc^{1/3}, \quad (23)$$

for an open pipe flow.

If β is used to substitute the mass transfer coefficient K , we obtain

$$Sh_{\beta} = 0.3825Re^{0.60}Sc^{1/3}(d/L)^{1/3} \quad (24)$$

for a closed loop flow. The above two equations indicate both forms of the Sherwood number have the same scaling with the Schmidt number. The dependence of Reynolds number for the mean corrosion in a pipe flow is $Re^{0.860}$ and for the corrosion in a closed loop flow is $Re^{0.6}$. Eq. (24) is obtained based on the assumption that the axial velocity is linear in the transverse coordinate y in the mass transfer boundary layer, therefore it should be valid for high Sc number cases.

Two configurations are considered in the present study: a closed loop flow and an open pipe flow. The mean corrosion/precipitation rate for a closed loop flow is zero, meaning that it is the temperature gradient that sustains the corrosion process and precipitation is important. Corrosion in an open pipe flow is higher than that in the closed loop flow. The present model indicates that the corrosion rate in a non-isothermal system is composed of two parts: the mean part due to mean surface concentration and the varying part due to the axial surface concentration profile. The second part is proportional to $L^{-0.333}$, indicating that the pipe length affects corrosion rate profile in a non-isothermal pipe flow system through temperature gradient. Fig. 6 shows the variations of the corrosion rate profile with varying L . Other parameters are the same to that in the MTL loop (Section 3). The figure shows that the corrosion rate at the highest temperature leg increases with the decreasing length. We find precipitation for $d/L = 0.01$ and

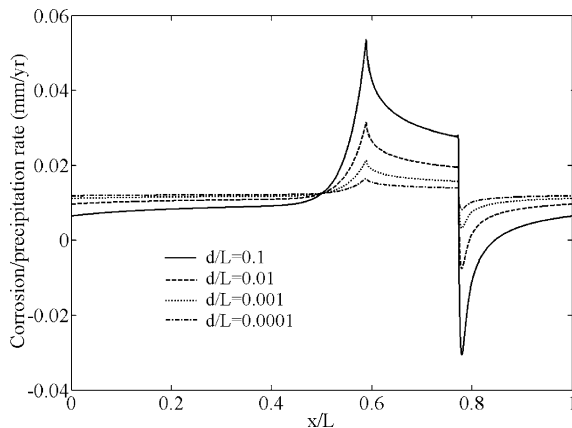


Fig. 6. Pipe length effects on the corrosion/precipitation rate profile in a non-isothermal pipe flow ($T_{\max} = 550$ °C, $T_{\text{int}} = 450$ °C and $T_{\min} = 350$ °C).

$d/L = 0.1$ that locates shortly after the highest temperature leg.

The present study is confined to the constant hydraulic parameter cases, i.e. the hydraulic parameters do not change in the flow direction. In future studies, loops of multi-modules and multi-branches shall be included. Other challenges in future work are the modeling of the chemical reaction kinetics of the corrosion products and oxygen in the bulk flow and transient corrosion/precipitation process, in which the initial impurities, such as iron in LBE should be considered.

Finally, the present model is only valid for the high Schmidt number flow, i.e. liquid metal flow, in which the mass diffusion layer is submerged under the hydraulic boundary layer. For small and intermediate Schmidt numbers, more sophisticated models are necessary to analyze the corrosion/precipitation phenomena.

5. Conclusions

The analysis of this corrosion model reveals three important attributes. First, the corrosion rate depends not only on the local temperature and flow conditions, but also on the axial temperature profile. Second, in the non-isothermal closed loop flow, the local corrosion rate scales as $Re^{0.60}$ and $Sc^{0.333}$. Third, for a closed loop flow, the mean corrosion rate is zero in the steady state and the local corrosion rate is smaller than that for pipe flow at the same condition. The non-local analyses show what the maximal corrosion and precipitation rates are and where they are located, and provide means to reduce and shift the locations through controlling the axial temperature profile.

For our LBE test loop, we find the highest corrosion rate at the beginning of the hot test section and the highest precipitation rate shortly after the hot test section. After the temperature gradient exceeds a certain level, the corrosion profile changes little with further increase of the gradient. The highest and the intermediate temperatures have significant effects on the corrosion magnitude at the test section. For accelerated corrosion test, it is necessary to increase the highest temperature while reducing the intermediate temperature. If possible the temperature gradient should be set close to 200 °C.

References

- [1] F. Balbaud-Celerier, F. Barbier, J. Nucl. Mater. 289 (2001) 227.
- [2] L.F. Epstein, Liquid Metals Technol. 20 (1957) 67.
- [3] J. Sannier, G. Santarini, J. Nucl. Mater. 107 (1982) 196.
- [4] X. He, N. Li, M. Mineev, J. Nucl. Mater. 297 (2001) 214.

- [5] V. Tcharnotskaia, C. Ammerman, T. Darling, J. King, N. Li, D. Shaw, L. Snodgrass, K. Woloshun. Liquid Lead–Bismuth Materials Test Loop, Proceeding of ADTTA/AccApp'01, 2001.
- [6] N. Li, *J. Nucl. Mater.* 300 (2002) 73.
- [7] F.P. Berger, K.F.F.L. Hau, *Int. J. Heat Mass Transfer* 20 (1977) 1185.
- [8] J. Zhang, N. Li, *Nucl. Technol.*, in press.